Water Science & Technology

Water Science & Technology Vol 00 No 0, 1 doi: 10.2166/wst.2023.052

Dam failure analysis and flood disaster simulation under various scenarios

Yasin Paşa [a], İsmail Bilal Peker [b], Abdülbaki Hacı [b] and Sezar Gülbaz [b,*]

[a] Department of Civil Engineering, Istanbul Gelişim University, Avcılar, Istanbul 34310, Türkiye
[b] Department of Civil Engineering, Istanbul University-Cerrahpaşa, Avcılar, Istanbul 34320, Türkiye
*Corresponding author. E-mail: sezarg@iuc.edu.tr

YP, 0000-0003-2104-9746; İBP, 0000-0001-9133-6797; AH, 0000-0003-3409-2209; SG, 0000-0002-2274-6896

ABSTRACT

The aim of this study is to analyze the effects of a possible dam failure under various scenarios and to generate a flood hazard map for two consecutive dams located in a study area with a dense-residential region and a heavy-traffic highway. Two consecutive dams consist of Elmalı 2, a concrete-buttress dam and Elmalı 1, an earth-fill gravity dam in the upstream and downstream, respectively. Hydrologic Engineering Center-River Analysis System (HEC-RAS) was used to develop a dam failure model. Dam failure scenarios were examined regarding three main criteria: the Breach Formation Time (BFT), the Number of Failed Buttresses (NFB) of Elmalı 2, and the Reservoir Volume Ratio (RVR) of Elmalı 1. Accordingly, flood peak depth (H_p), peak flow rate (Q_p), peak velocity (v_p), and time to reach the peak (t_p) are discussed. The results showed that BFT and NFB of Elmalı 2 were highly effective on these values, whereas RVR of Elmalı 1 had no significant effect. Moreover, the total area affected by potential floods was calculated with a comparative areal change analysis using flood inundation and flood hazard maps obtained. Estimated damage costs indicate that in the worst-case scenario, more than 500 buildings will be affected in the region.

Key words: buttress dam, consecutive dams, dam failure analysis, flood hazard map, HEC-RAS

HIGHLIGHTS

- The effects of a possible dam failure on two consecutive dams are analyzed.
- The study focuses on the dam failure analysis of a concrete-buttress dam located on a high-density residential area and a heavy-traffic highway, which is different among dam failure studies.
- Flood inundation and hazard maps for the study area are generated.
- The results obtained in this study serve as a guide for those living downstream of the Elmalı dam in the future.

GRAPHICAL ABSTRACT

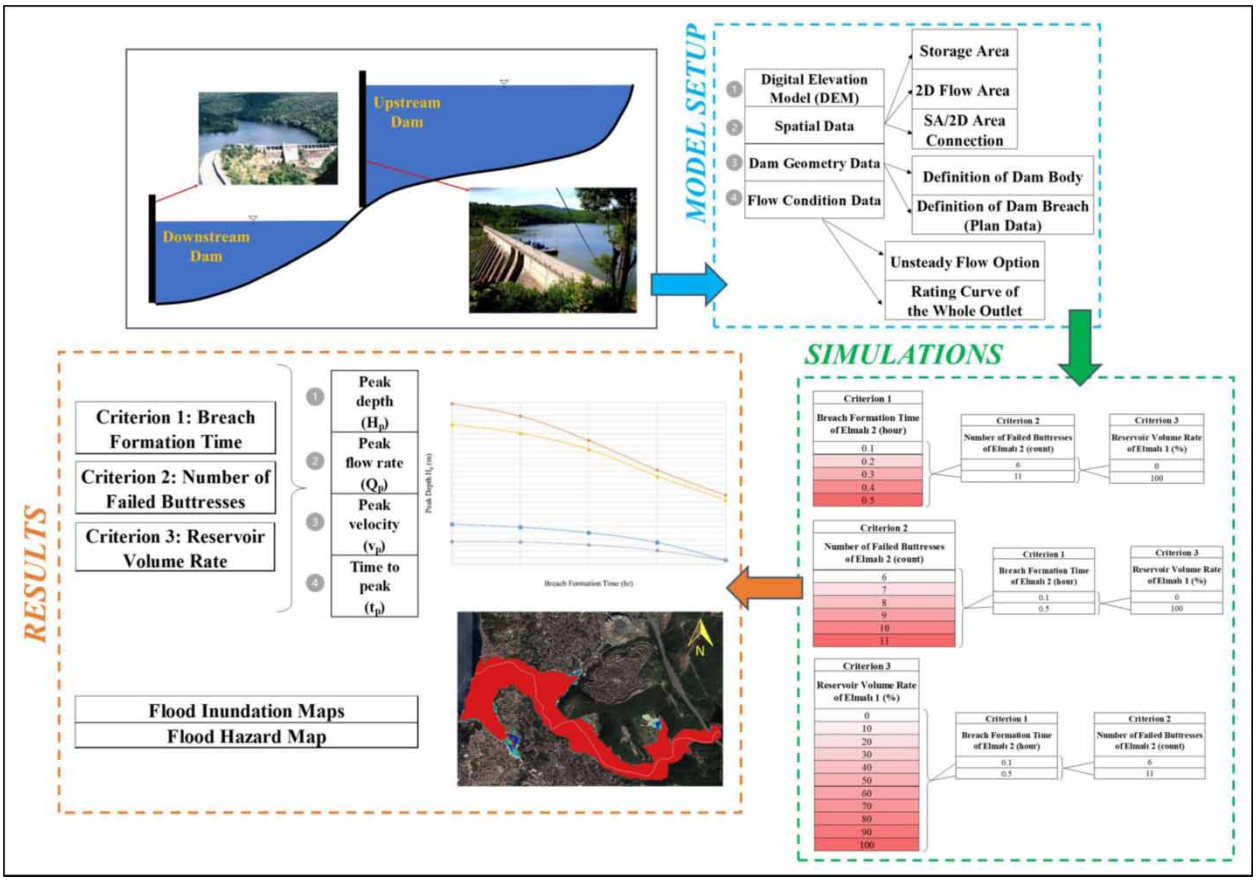

1. INTRODUCTION

Despite many benefits such as water supply, irrigation, and power generation, full or partial failure of dams due to various reasons poses risks for people (Altinbilek 2002). Regardless of dam type and breach formation in the dam body, a catastrophic dam failure leads to uncontrolled and massive flooding downstream, even a flood wave propagates in a short time and destroys the settlements it encounters. Compared to other types of disasters, floods resulting from dam failures are the most destructive events in terms of the number of casualties and value of property loss. More than one hundred dam failures have occurred since the 1700s and thousands of people have died in addition to environmental damages worldwide (Foster *et al.* 2000; Zhang *et al.* 2009; Petaccia *et al.* 2016).

Failure of a dam occurs for different reasons, like seepage, piping, overtopping, earthquake, landslide, and foundation failure or sabotage (Wu 2011; Brunner 2014). The main causes of dam failure are overtopping and piping (Bosa & Petti 2013; Amini *et al.* 2017; Li *et al.* 2021). According to the reports (ICOLD 1998), about 38% of dam failures were caused by overtopping related to the inadequate spillway capacity. Also, about 33% of dam failures were related to seepage or piping. Even if the reason may vary, almost all dam failures begin with a breach formation (Xiong 2011). A breach is defined as an opening formed in the dam body and its gradual expansion results in the destructive propagation of the large volume of water in the reservoir to the downstream (Wahl 1998). Breach geometry (e.g., breach depth, width, and breach side slope factor), timing (initial breach time, Breach Formation Time (BFT), etc.), failure mode, and breach progression need to be estimated precisely in dam failure modeling (Froehlich 2008). Also, flow conditions and dam body type can affect estimating the peak hydrograph, which occurs after the breach progression (Brunner 2014). Consequently, there are two fundamental tasks in dam failure analysis: prediction of reservoir outflow hydrograph and hydrograph routing for this through downstream (Wahl 1998).

Since the collapse of a dam directly affects many people's lives, dam failure analysis and flood area modeling studies become critical. Therefore, researchers utilize several dam failure simulation programs in various regions of the world (Bozkus & Bag 2011; Singh *et al.* 2011; Cannata & Marzocchi 2012; Qi & Altinakar 2012; Alvarez *et al.* 2017; Kumar *et al.* 2017; Sawai *et al.* 2019). The most commonly used programs are DAMBRK (The Dam Break Model) (Fread 1984), MIKE (DHI 2017), and HEC-RAS (Hydrologic Engineering Center-River Analysis System) (USACE 2016). In addition to these, a physical-based dam breach model named DB-IWRH (Dam Break-Institute of Water Resources and Hydropower Research) is utilized for analysis (Yu *et al.* 2021). HEC-RAS was used as an effective tool in many studies examining dam failures (Butt *et al.* 2013; Haltas *et al.* 2016; Balogun & Ganiyu 2017; Joshi & Shahapure 2017; Sharma & Mujumdar 2017; Yakti *et al.* 2018; Albu *et al.* 2019, 2020; Kilania & Chahar 2019; Aribawa *et al.* 2021). The flood depth calculated at the downstream of Um Al-Khair Dam by using the HEC-RAS program was compared to the observed water depth at the known location during the dam break event (Azeez *et al.* 2020). In this study, the authors obtained a reasonable amount of correlation between the observed and the calculated depths. In these studies, inundation, hazard maps, or flood hydrographs created by dam failures were generated in different critical regions around the world, which can be dangerous to human life in place like villages on the downstream area of a dam. Also, there is a consensus on the powerful modeling capability of HEC-RAS two dimensional (2D) in dam failure analysis. Accordingly, HEC-RAS 2D is preferred in the current study for generating and analyzing flood simulations due to its greatly enhanced modeling and predicting capacity, alongside the fact that downloading and using it is free.

The primary purpose of this study is to reveal and evaluate the flood inundation and hazard maps that may occur due to possible dam failure scenarios in Istanbul, Türkiye. The results are evaluated for the study area, including highly-populated residential areas, a heavy-traffic highway, downstream of consecutive dams, Elmalı 2, and Elmalı 1. Dam failure simulations were performed with three criteria: BFT, Number of Failed Buttresses (NFB) of Elmalı 2 and Reservoir Volume Ratio (RVR) of Elmalı 1. The simulations were performed as 88 runs under three different simulation sets based on these criteria. Simulation results provide information such as the peak flood depth, flow rate, flood velocity, time to reach the peak, and flood maps for the likely scenarios. Flood maps obtained in the simulations were compared spatially and the effects of the three criteria on the flood were analyzed. Additionally, the present study aims at discussing the consequences of possible dam failure disasters in the study area under different criteria by examining the simulation results. Evaluating the effects of different criteria on flood parameters is essential for the operation of dams and taking the necessary measures to minimize the harmful effects of a dam failure. Moreover, identifying the flood-susceptible areas is of great importance in taking proper precautions to mitigate flood hazards.

2. MATERIALS AND METHODS

2.1. Study area

The study area is located in Istanbul, Türkiye, as shown in Figure 1. Among the residential areas around the Göksu River flowing into the Bosphorus, those located in the downstream area of the dams are at risk of flooding (Figure 1). There are two dam bodies: the first one, Elmalı 1, was operationalized in 1907 and the second one, Elmalı 2 was constructed in 1955. Elmalı 2 is located 1.2 km upstream of the first dam. Elmalı 1 is an earth-fill gravity dam with a body height of 22 m. Elmalı 2 is a buttress dam with a body height of 49 m. The total drainage area of the two dams is 81.5 km^2. The maximum water surface elevations of the dams are 32.4 m and 67.5 m for Elmalı 1 and Elmalı 2, respectively. At these water surface elevations, the reservoir storage capacities are 1.7 and 17.0 $\times$ 10^6 m^3 for Elmalı 1 and Elmalı 2, respectively (Mahnamfar *et al.* 2020). The main focus of this study is the possible destruction of the buttresses of the Elmalı 2 since Elmalı 1 has a lower storage capacity and flood risk.

In Figure 2, the cross-sections of the dam bodies are given. The detailed geometric specifications of the dam bodies are presented in Table 1. The downstream of Elmalı 2 is selected as the study area for the flood risk analysis because the dams are in a critical metropolitan region of Istanbul with a high population density. The approximate population living downstream of these two consecutive dams is 40,000. Additionally, there are many industrial, commercial, and historical structures, as well as the TEM (Trans European Motorway) highway and Küçüksu Pavilion. Any possible failure of these dam bodies is expected to cause severe damage to the residential area and the bridge piers of the TEM highway. Accordingly, these two consecutive dams were the focus because Elmalı 2, a concrete-buttress dam close to a dense-residential area and a heavy-traffic highway, makes this study different among traditional dam failure studies.

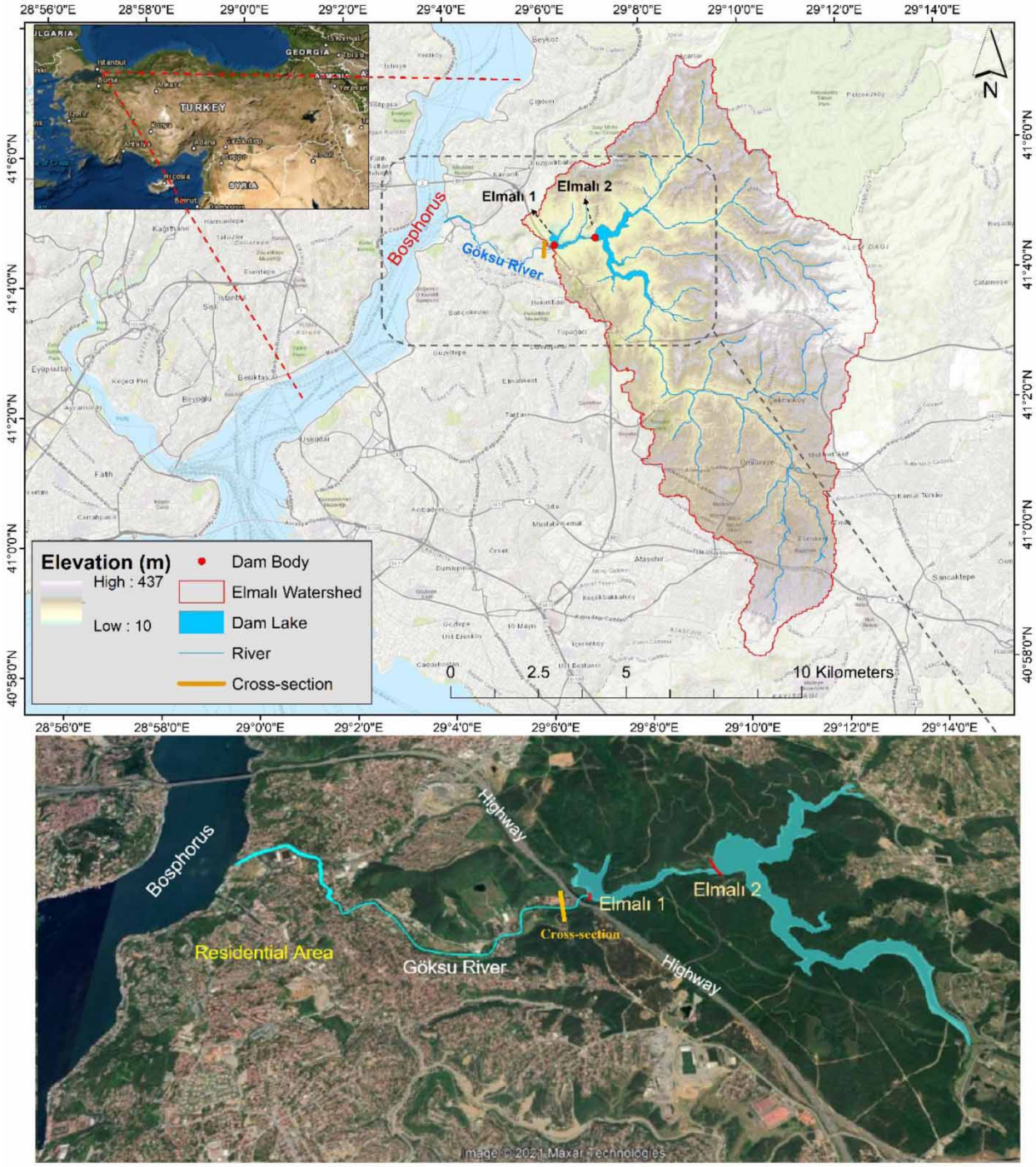

Figure 1 | Location of Elmalı 1 and Elmalı 2 with the drainage area and the stream network.

2.2. Methodology and data

HEC-RAS software version 5.0.7 was used for the dam failure analysis of Elmalı 2 with the 2D unsteady flow for the selected study area. HEC-RAS 2D is a powerful yet easy-to-use software for determining water depth, flow rate, inundation area, flood velocity, and water surface profile in 2D (Joshi & Shahapure 2017). The 2D flood models can simulate water flow in both longitudinal and lateral directions and these models represent the terrain as a continuous surface through a mesh or grid. Therefore, this study was performed using the 2D model to generate reliable inundation mapping and flood wave analysis.

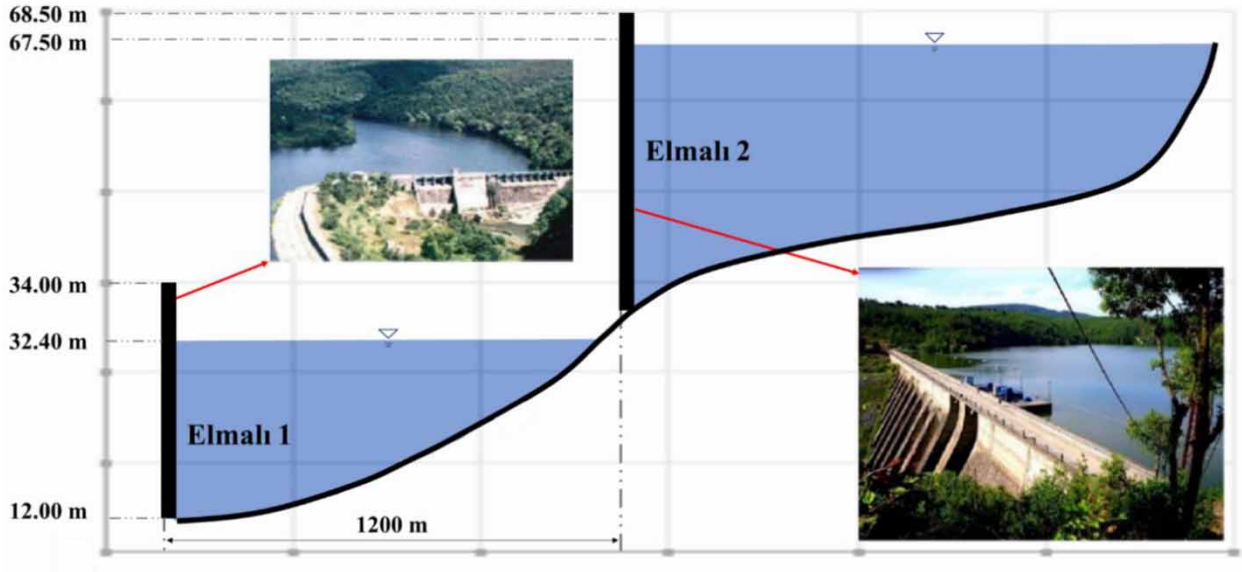

Figure 2 | The crest and water surface elevations and general view of Elmalı 1 and Elmalı 2 consecutive dams.

Table 1 | Main properties of Elmalı 1 and Elmalı 2 dam bodies

	Elmalı 1	Elmalı 2
Dam type	Earth-fill gravity	Concrete-buttress
Spillway type	Sluice gate: 11 openings	Radial gate: three openings
Height from the foundation level	22.0 m	49.0 m
Crest elevation	34.0 m	68.5 m
Maximum water surface elevation	32.4 m	67.5 m
Crest length	298.4 m	238.8 m
Crest width	3.3 m	4.6 m
Upstream side slope	–	0.4
Downstream side slope	–	0.6

The HEC-RAS model was comprised of three main components: geometric data, flow data, and plan data. Required data were obtained from the General Directorate of State Hydraulic Works (DSI) and Istanbul Water and Sewerage Administration (ISKI). The unsteady flow simulation was performed with the geometric data using the Digital Elevation Model (DEM), which has a 1 m resolution obtained from the Republic of Türkiye-Ministry of National Defense General Directorate of Mapping (HGM). The HEC-RAS program solves all 2D Saint-Venant equations shown in Equations (1)–(3) (Brunner 2014):

Continuity equation:

$$\frac{\partial \zeta}{\partial t}+\frac{\partial p}{\partial x}+\frac{\partial q}{\partial y}=0 \tag{1}$$

Momentum equation:

$$\frac{\partial p}{\partial \tau}+\frac{\partial}{\partial x}\left(\frac{p^2}{h}\right)+\frac{\partial}{\partial x}\left(\frac{pq}{h}\right)=-\frac{n^2 pg\sqrt{p^2+q^2}}{h^2}-gh\frac{\partial \zeta}{\partial x}+pf+\frac{\partial}{\rho\partial x}\left(h\tau_{xx}\right)+\frac{\partial}{\rho\partial y}\left(h\tau_{xy}\right) \tag{2}$$

$$\frac{\partial p}{\partial \tau}+\frac{\partial}{\partial y}\left(\frac{q^2}{h}\right)+\frac{\partial}{\partial x}\left(\frac{pq}{h}\right)=-\frac{n^2 qg\sqrt{p^2+q^2}}{h^2}-gh\frac{\partial \zeta}{\partial y}+qf+\frac{\partial}{\rho\partial y}\left(h\tau_{yy}\right)+\frac{\partial}{\rho\partial x}\left(h\tau_{xy}\right) \tag{3}$$

where h is the water depth (m), p and q are the specific flows in the x and y directions (m^2s^{-1}), respectively, ζ is the surface elevation (m), g is the gravitational acceleration (ms^{-2}), n is the Manning resistance, ρ is the water density (kgm^{-3}), τ_{xx}, τ_{yy}, and τ_{xy} are the components of the effective shear stress, and f is the Coriolis force (s^{-1}).

2.3. Dam failure scenarios

To construct HEC-RAS 2D models, the dam was represented as a Storage Area/2D Area Connection (SA/2D AC). This allows the user to enter pre-determined breach data for estimating breach parameters. It is challenging to predict dam failure risk as dam breach parameters and breach failure time cannot be predicted by any commercially available mathematical model. The development of the breach is idealized as a parametric process because it cannot be simulated in any physical sense. Therefore, a dam failure is defined by the shape and size of the breach and the time required for its development, which is called BFT (Wahl 2004). Petrascheck & Sydler (1984) stated that breach size and BFT have significant effects on flood flow rate, flood depth, and time to reach the peak. Moreover, some structures, such as dam reservoir and natural or artificial lakes affect the damages of the flood that may occur as a result of dam failure (RCEM 2015; Duchan *et al.* 2020). Therefore, estimation of a dam failure flood disaster depends on these parameters. In our study, BFT, size of the breach defined as NFB and the reservoir volume ratio of Elmalı 1 (RVR) are used to estimate floods due to dam failure. In the dam failure scenarios, three different criteria were analyzed regarding the probability of Elmalı 2 dam failure: BFT and NFB of Elmalı 2 and RVR of Elmalı 1. The simulations were based on the failure of the buttresses of Elmalı 2 under various scenarios. Since the main focus was the destruction of the buttresses of the Elmalı 2, the RVR of Elmalı 1 was considered as a criterion for failure scenarios. This study did not focus on the failure analysis of Elmalı 1 because it is operationally empty. Failure simulations are carried out for the critical upstream dam Elmalı 2. The RVR of the downstream dam Elmalı 1 is considered as a scenario criterion only. The RVR criterion can only be observed when the overflowing water reaches Elmalı 1 after Elmalı 2 is completely filled. Therefore, all scenarios for Elmalı 1 were invariably generated for a trapezoidal breach shape of 2:1 and a BFT of 0.25 h.

The flow chart of the modeling process is shown in Figure 3. After the model was setup using the required inputs, the simulations were derived for scenarios based on three main criteria and the effect of each was investigated in the cross scenarios. For the first criterion, in accordance with the values reported in the literature (USACE 1980), the effect of the BFT was evaluated by increasing from 0.1 to 0.5 h (0.1 h each run). However, the minimum and maximum values of the other two criteria were kept constant in the combinations performed. Accordingly, limit values of 0–100% were used for the RVR of Elmalı 1; NFB was selected between 6 and 11. It should also be noted that although there are a total of 16 buttresses in the Elmalı 2 dam body, the number of breached buttresses in the scenarios was determined as 6–11, in accordance with the values reported in the literature (ANCOLD 2012; Pilotti *et al.* 2020). In the simulations, 6–11 buttresses represent the breached parts of the dam body. Therefore, a simulation set consisting of 20 runs based on the variation of the first criterion was performed. Similarly, other scenarios were also examined to analyze the variation of the second and third criteria. For the second criterion, the NFB was increased from 6 to 11 (one buttress per run), and the other criteria were kept at their limit values (0–100% for the RVR of Elmalı 1 and 0.1–0.5 h for the BFT). Hence, a second simulation set consisting of 24 runs based on the variation of the second criterion was performed. Finally, the third criterion (RVR of Elmalı) was examined by increasing RVR from 0 (empty) to 100% (full) (10% increase each run) and the others were kept at limit values (6–11 failed buttresses and 0.1–0.5 h for the BFT). Therefore, a third scenario set of 44 runs was created to examine the effect of the last criterion. Three different simulation sets were analyzed for a total of 88 runs. The scenarios are shown in the flow chart of the modeling process in Figure 3.

Results were obtained by examining the hydraulically essential parameters for a flood disaster. Parameters indicating the degree of severity and risk of the destructive effect resulting from dam failure were identified as the peak values of water depth, flow rate, and velocity. Moreover, the reach time to the peak values was monitored. In simulations, variations in these parameters were examined temporally during the analysis period. In addition, flood maps were constituted for visual evaluations of the regions that might be affected by a possible dam failure. Hence, the areas affected by the dam failure flood were evaluated spatially.

3. RESULTS

The model results were discussed under three criteria, the effects of the BFT and the NFB of Elmalı 2 and the RVR of Elmalı 1, which are considered to be effective in a dam failure. The simulations were performed as 88 runs under three different

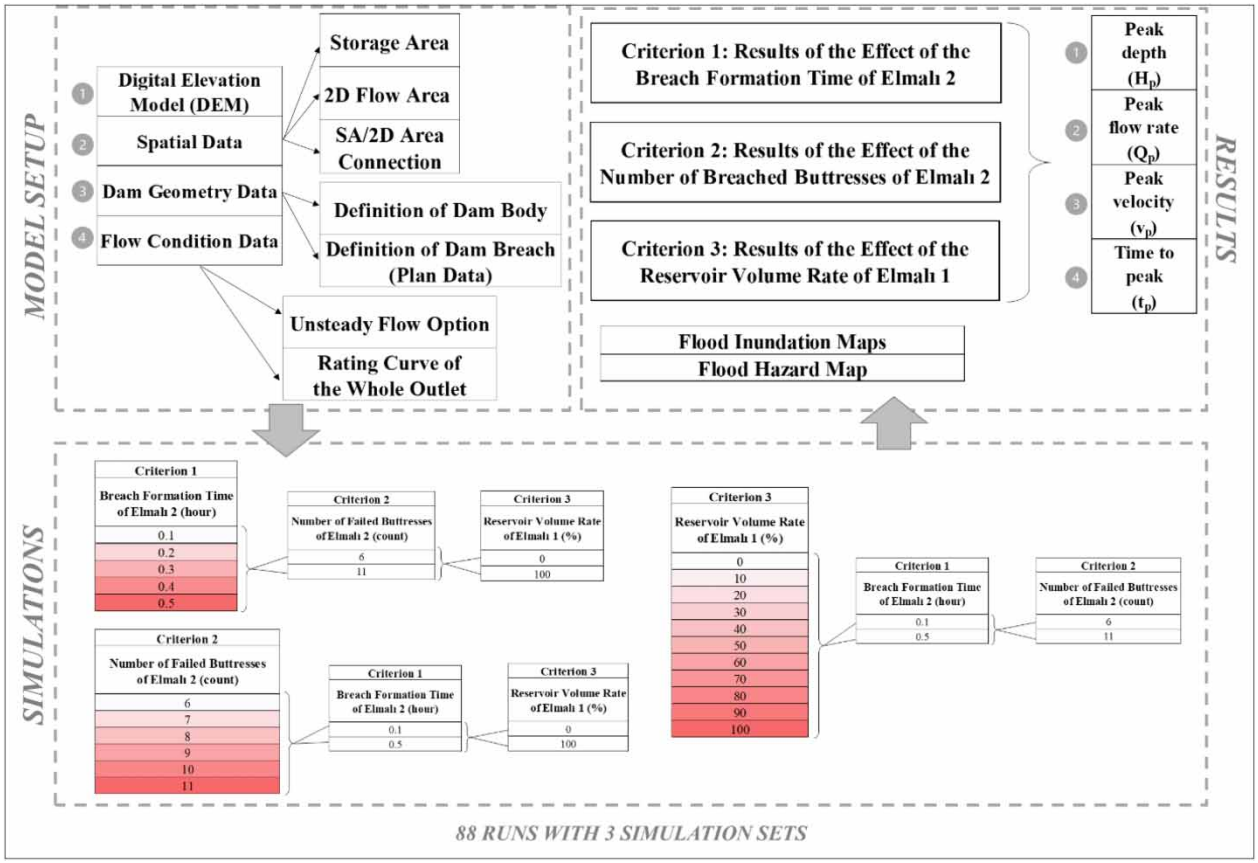

Figure 3 | The flow chart of the modeling process.

simulation sets based on these criteria. Therefore, 88 flood hydrographs, depths, and velocity curves were obtained from the model for each scenario. The peak values of flow rate, water depth, and velocity in the curves were used to examine the effects of three criteria. Moreover, the reach time to the peak values was monitored in the model. The model results are presented as four different outputs: peak values of the flood depth (H_p), flow rate (Q_p), velocity (v_p), and time to reach the peak (t_p). The model outputs were obtained from the cross-section in the downstream area of the Elmalı 1 dam body seen in Figure 1. Hence, the effects of three different criteria were investigated on the graphs comparatively. Also, as a spatial output of the flood due to a possible failure, flood inundation, and hazard maps were generated for the study area. Furthermore, the hazard caused by the dam failure flood was calculated using the flood maps generated.

3.1. Effect of the breach formation time (Criterion 1)

The failure process of Elmalı 2 was analyzed for various BFTs, which ranged between 0.1 and 0.5 h (0.1 h each time). In this analysis, four different model outputs emerged by evaluating the limit values of the other two criteria (6–11 for NFB and 0–100% for RVR of Elmalı 1). Thus, the effect of the BFT was examined by comparing the sudden and slow failure scenarios. As a result, Figure 4(a) points out that the peak depth values gradually decrease while the BFT increases for all other criteria. Similarly, the peak velocity and the peak flow values also decreased as BFT increased from 0.1 to 0.5 h, as shown in Figures 4(b) and (c), respectively.

To observe the effect of the BFT, the change in the limit values of Criterion 3 (RVR of Elmalı 1) was analyzed while the NFB values (Criterion 2) were kept constant. Accordingly, for Criterion 1, as the RVR values for Elmalı 1 is empty (0%) and full (100%), a decline in the peak flow of 8–14% was observed for the scenario with six failed buttresses and a decline of 29–36% was obtained for 11 failed buttresses. Comparatively, the RVR of Elmalı 1 had less impact on the peak flood results. In the fastest failure scenario, the difference between peak values for the RVR of Elmalı 1 was small (around 5% in peak flow and 1–2 mn in time to peak) and the difference between peak values decreased as the BFT increased. The results

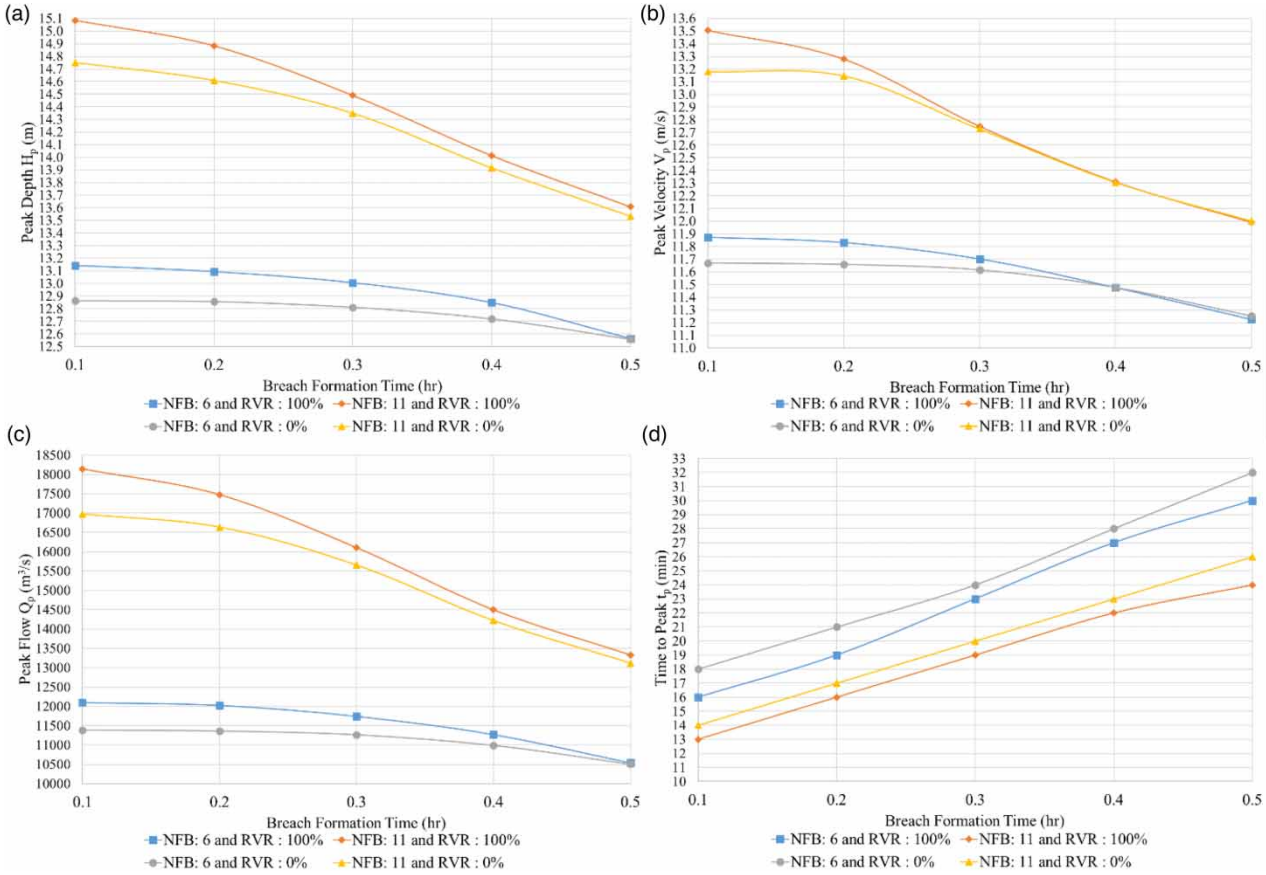

Figure 4 | Variation of (a) the peak depth; (b) the peak velocity; (c) the peak flow; and (d) the time to peak according to different BFTs.

were almost similar in the slowest failure scenario, regardless Elmalı 1 was empty or full. On the other hand, the time to peak values naturally rise with the increasing BFT (Figure 4(d)). In the slow failure scenario (for 0.5 h), a delay of 11–14 min was observed in the time to reach the peak values compared to the sudden failure scenario (for 0.1 h).

3.2. Effect of the number of failed buttresses (Criterion 2)

The failure scenarios for Elmalı 2 were examined for different NFB values varying from 6 to 11. With this analysis, the change in peak values was examined for different numbers of failed buttresses. The effect of the NFB was examined in 24 different situations using the limit values of the other two criteria. In simulations, the peak depth, peak velocity, and peak flow increase proportionally with the NFB, as shown in Figure 5(a) and (c), respectively. For both limit values of Criterion 3 (0–100%), the rate of increase in the peak flow was approximately 33% for the 0.1 BFT scenarios and around 20% for the 0.5 BFT scenarios. Cases, where Elmalı 1 is empty (0%) or full (100%), gave similar results under various scenarios of the NFB. In the slow failure scenario, cases where RVR of Elmalı 1 was empty or full gave almost similar results for different NFB values. This difference was slightly higher for the sudden failure scenario, but it was still found to be minor considering the other criteria. On the other hand, time to peak values decreased as the NFB increased (Figure 5(d)). Comparing the limit values at which 6 and 11 buttresses collapsed, the delay in the time to peak was 3 min in sudden failure and 6 min in slow failure.

3.3. Effect of the reservoir volume ratio of Elmalı 1 (Criterion 3)

In order to scrutinize the effect of various RVR for Elmalı 1, 44 different simulations were performed using the limit values of the other two criteria. The analysis results revealed that the RVR of Elmalı 1 was an ineffective factor. As shown in Figures 6(a)–(d), the peak values (peak depth, peak velocity, peak flow, and time to peak) were not significantly affected by the change of this factor. The graphs formed almost horizontal lines. Thus, as a general statement for all the other

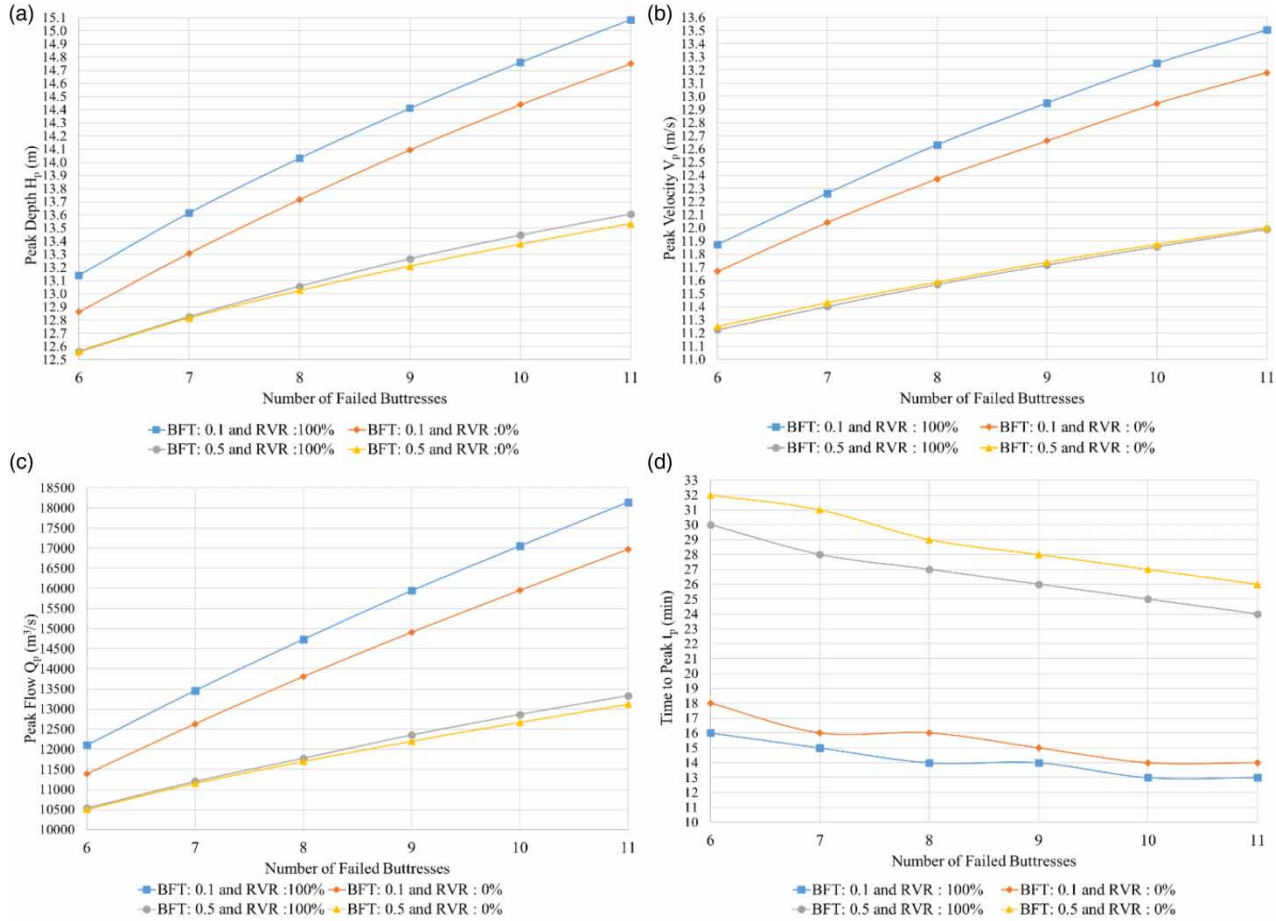

Figure 5 | Variation of (a) the peak depth; (b) the peak velocity; (c) the peak flow; and (d) the time to peak according to different NFB.

conditions, the water volume in Elmalı 1 does not significantly alter the flood peak values in any of the possible dam failure scenarios.

3.4. Flood inundation maps

In this part of the study, the change of inundation area for the three criteria under various scenarios and their impacts were analyzed on the model. For this purpose, the effect of the change in each criterion on the inundation area was determined. Table 2 shows the effect of different values of the three criteria on the change of the inundation area. For this analysis, the areal changes were reported by combining the limit values of the three criteria. For example, by changing the limit values of BFT (0.1–0.5 h), the flood inundation area in the 0.1 BFT scenario is 4.8% less than in the 0.5 BFT scenario, when observed for the scenarios with the constant values of NFB and RVR (six buttresses and 100% volume ratio). Accordingly, Criterion 2 was found to have the highest impact on the inundation area (about 6.0–14.7%). The effect of Criterion 1 on the inundation area was also found to be similar to Criterion 2, but slightly less (about 2.8–12.7%). On the other hand, the effect of changes in Criterion 3 was relatively small (less than 2.1%) compared to the other two criteria. As a result, finding the third criterion as the least effective factor means that the full or empty state of Elmalı 1 reservoir does not have a significant effect on the size of the dam failure flood.

Different combinations of the three criteria for the failure of Elmalı 2 were also investigated with flood inundation maps, thus flood-affected areas were visually identified under various scenarios. Figures 7–9 show the flood inundation areas with the flood depths obtained by the simulations for the minimum and maximum values of the three criteria. It was observed that the flood depth rises up to 20 m in the Göksu River. As shown in the flood maps, the flood inundation occupies the densely populated residential area for all cases. These results indicate that the possible failure of Elmalı 2 will affect the

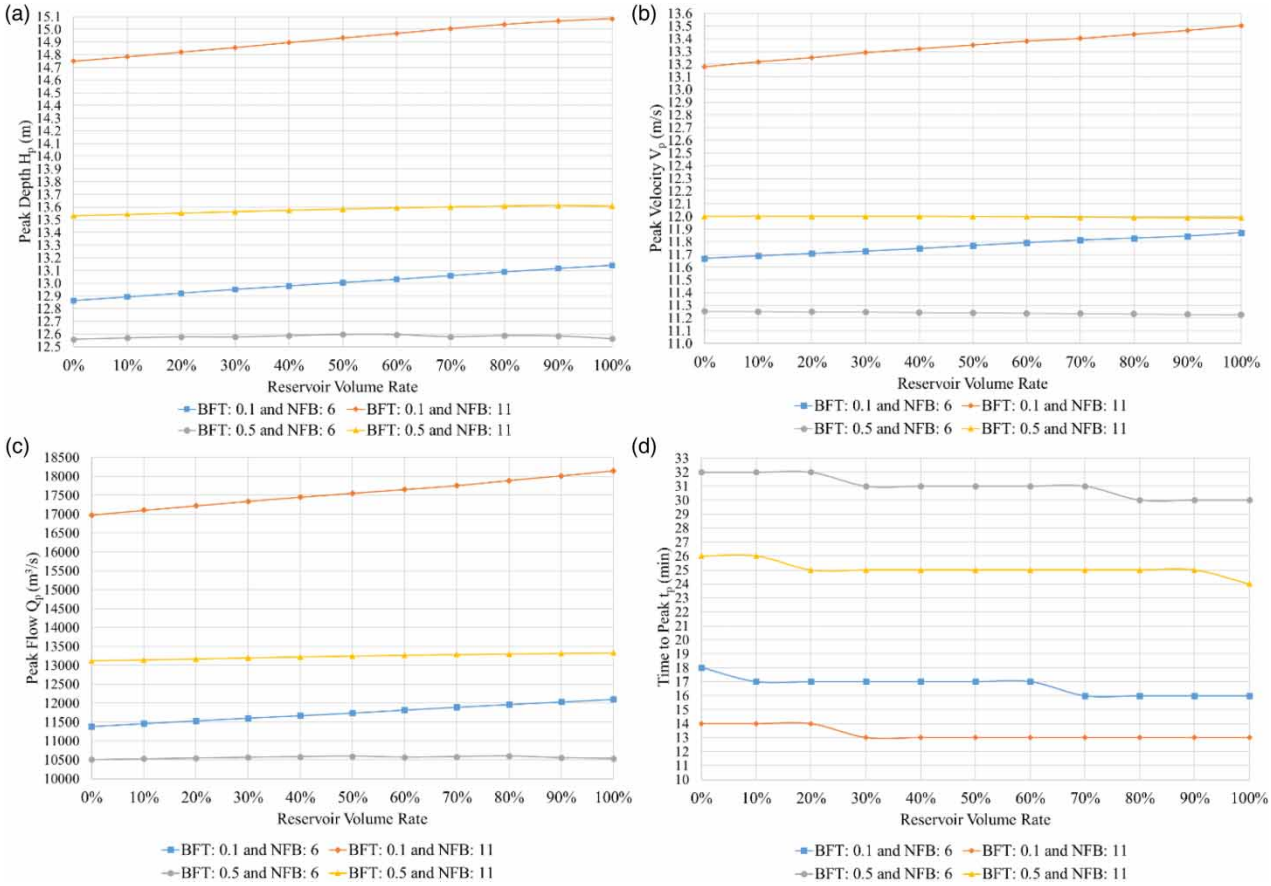

Figure 6 | Variation of (a) the peak depth, (b) the peak velocity, (c) the peak flow and (d) the time to peak according to different RVR of Elmalı 1.

flood-susceptible residential area. Figure 7 shows the flooded area difference between the sudden (BFT = 0.1 h) and slow (BFT = 0.5 h) failure scenarios. In Figure 7, there are four subfigures (A, B, C, and D), which correspond to the limit values of the other two criteria (6–11 for NFB and 0–100% for RVR of Elmalı 1). The effects of BFTs on flood inundation areas can be seen by comparing the flooded area difference in the same subfigure. It can be seen that the flooded area obtained from the model for the 0.1 h BFT scenarios is bigger than for the 0.5 h BFT scenarios. Figure 8 shows the impacts of NFB on flood inundation area by comparing the flooded area difference. It was obtained that the difference in the flooded area between 6 and 11 NFB is the highest. Figure 9 shows the impacts of RVR on flood inundation areas. The difference in the flooded area for RVR scenarios was relatively small compared to the other two criteria.

3.5. Flood hazard map

A flood hazard map was generated for the worst scenario, 0.1 h BFT, 11 NFB (Elmalı 2) and 100% RVR (Elmalı 1). This scenario yielded the largest inundation area. The flood depth for this scenario varied from 0 m to approximately 20 m in the downstream area of two consecutive dams. Flood zones were separated into five categories as 'very low', 'low', 'medium', 'high', and 'very high' according to the flood depth (Dinh *et al.* 2012). A flood depth greater than 2 m was considered a 'very high' hazard category. The other flood depth categories are given in Table 3. The areas for 'very low', 'low', 'medium', 'high', and 'very high' hazard categories were calculated as 18,000; 36,000; 40,000; 37,000; and 1,350,000 m^2 corresponding to 1.2, 2.4, 2.7, 2.5, and 91.2% of the total inundated area, respectively. The results showed that the major part of the study area was in the 'very high' hazard category and the downstream part of the consecutive dams has very high flood risk. The hazard zones for a possible dam failure are shown in Figure 10.

Table 2 | The effects of three criteria on the change of inundation area

Criterion 1	BFT of Elmalı 2	NFB of Elmalı 2	RVR of Elmalı 1	Areal Change (%)
	0.1	6	100	−4.8
	0.5	6	100	
	0.1	11	100	−12.7
	0.5	11	100	
	0.1	6	0	−2.8
	0.5	6	0	
	0.1	11	0	−11.3
	0.5	11	0	
Criterion 2	**NFB of Elmalı 2**	**BFT of Elmalı 2**	**RVR of Elmalı 1**	**Areal Change (%)**
	6	0.1	100	14.7
	11	0.1	100	
	6	0.1	0	14.4
	11	0.1	0	
	6	0.5	100	6.0
	11	0.5	100	
	6	0.5	0	6.3
	11	0.5	0	
Criterion 3	**RVR of Elmalı 1**	**BFT of Elmalı 2**	**NFB of Elmalı 2**	**Areal Change (%)**
	0	0.1	6	1.9
	100	0.1	6	
	0	0.5	6	0.4
	100	0.5	6	
	0	0.1	11	2.1
	100	0.1	11	
	0	0.5	11	0.1
	100	0.5	11	

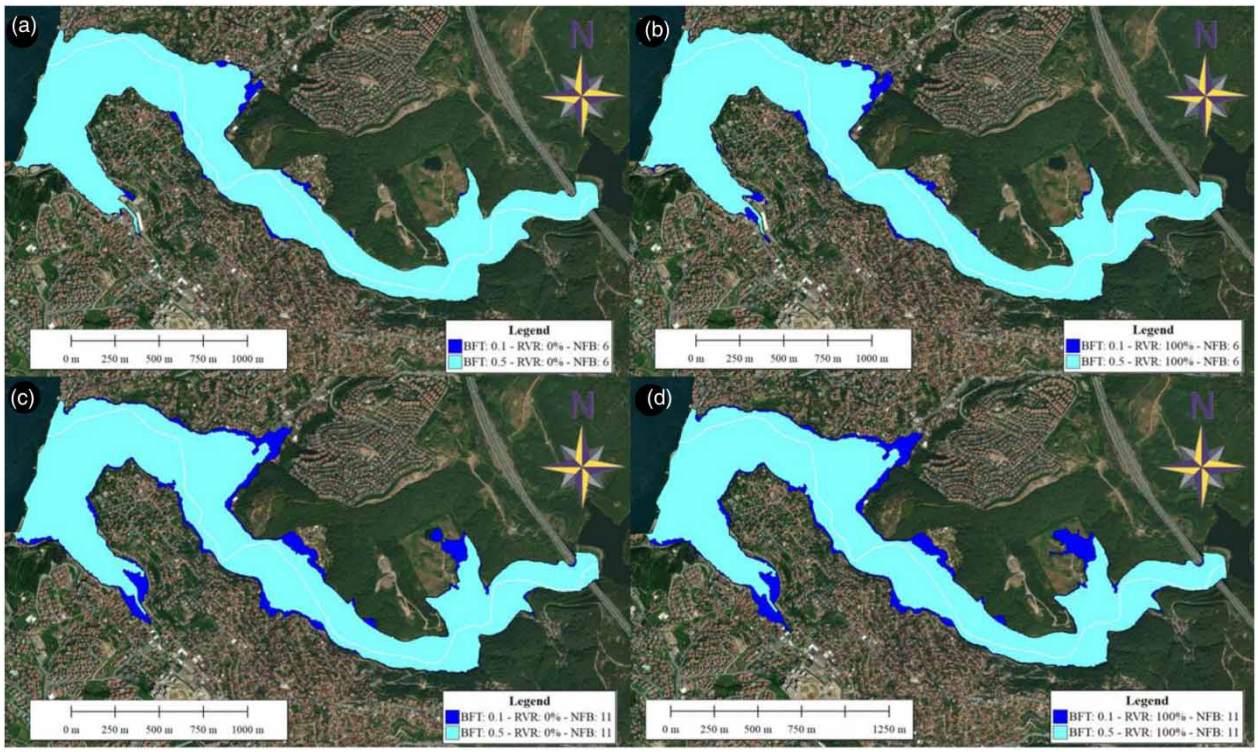

Figure 7 | Flood inundation maps by Criterion 1 showing the effect of BFT.

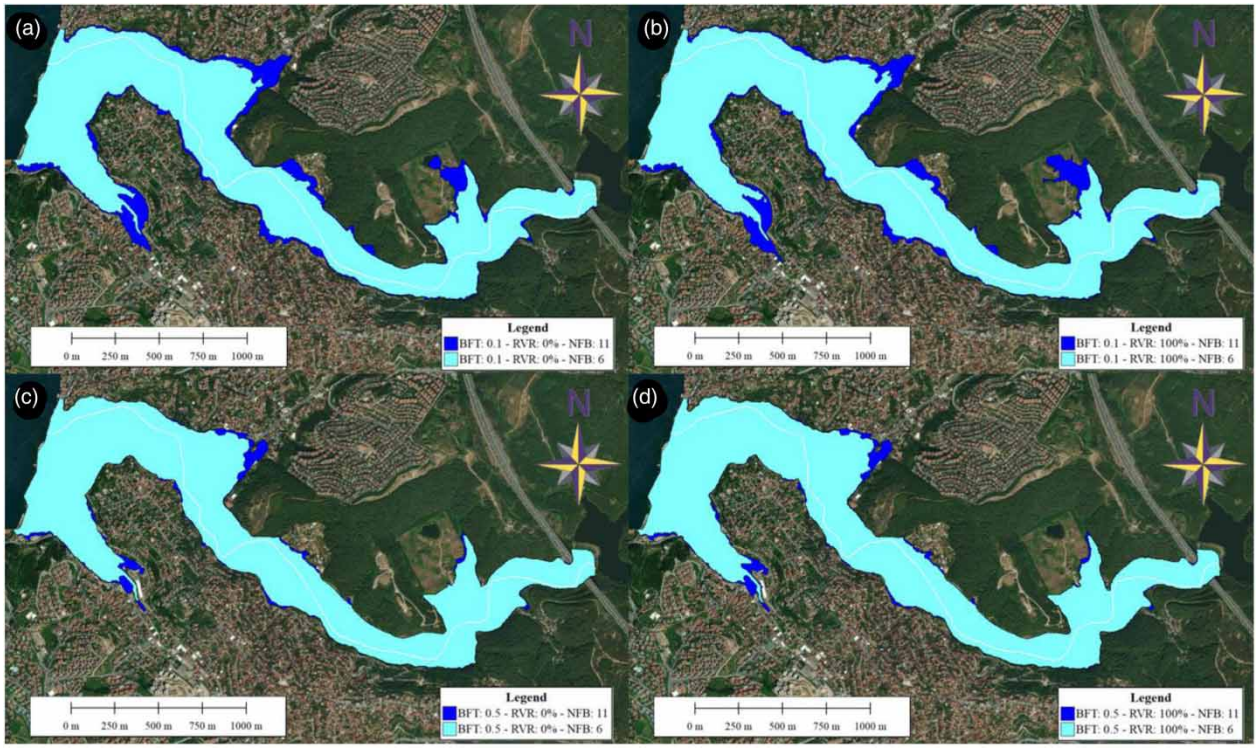

Figure 8 | Flood inundation maps by Criterion 2 showing the effect of NFB.

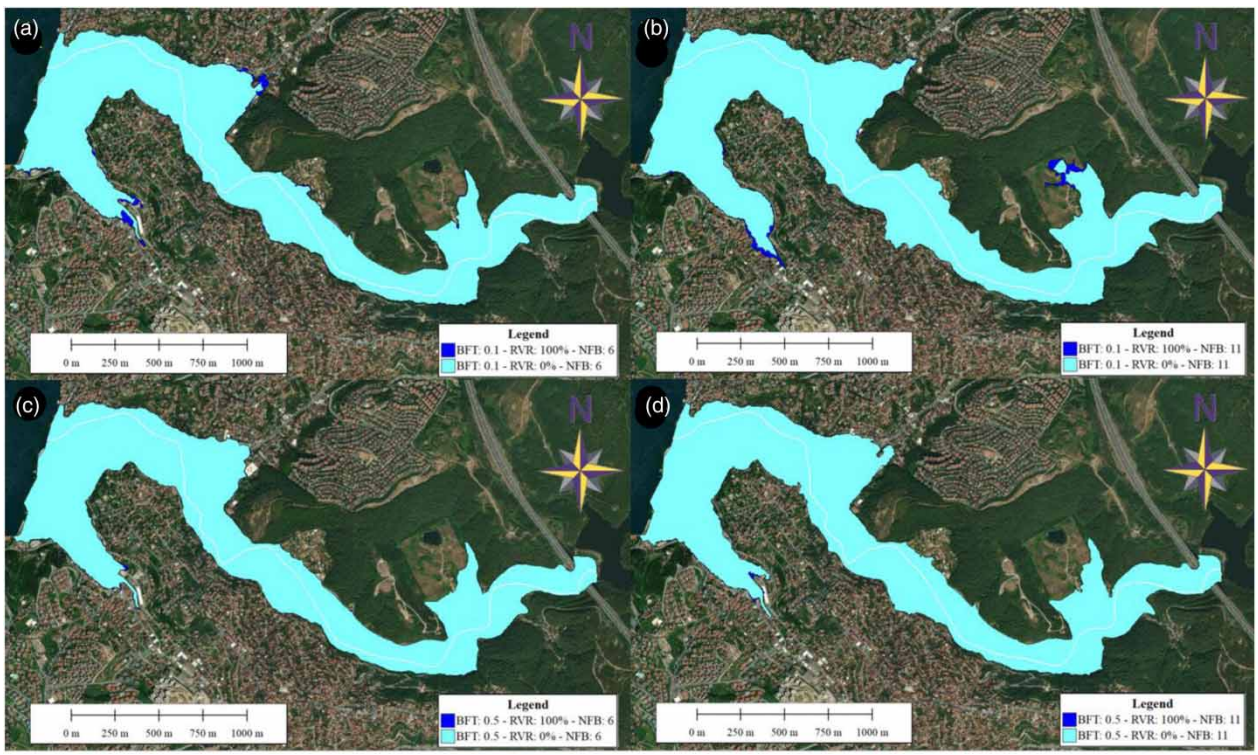

Figure 9 | Flood inundation maps by Criterion 3 showing the effect of RVR.

Table 3 | Hazard zones for the worst dam failure scenario

Flood depth (m) (Hazard zone)	Hazard zone area (m^2)	Percentage of hazard zone in the total inundated area (%)
0–0.2 (Very low)	18,000	1.2
0.2–0.5 (Low)	36,000	2.4
0.5–1.0 (Medium)	40,000	2.7
1.0–2.0 (High)	37,000	2.5
> 2.0 (Very high)	1,350,000	91.2

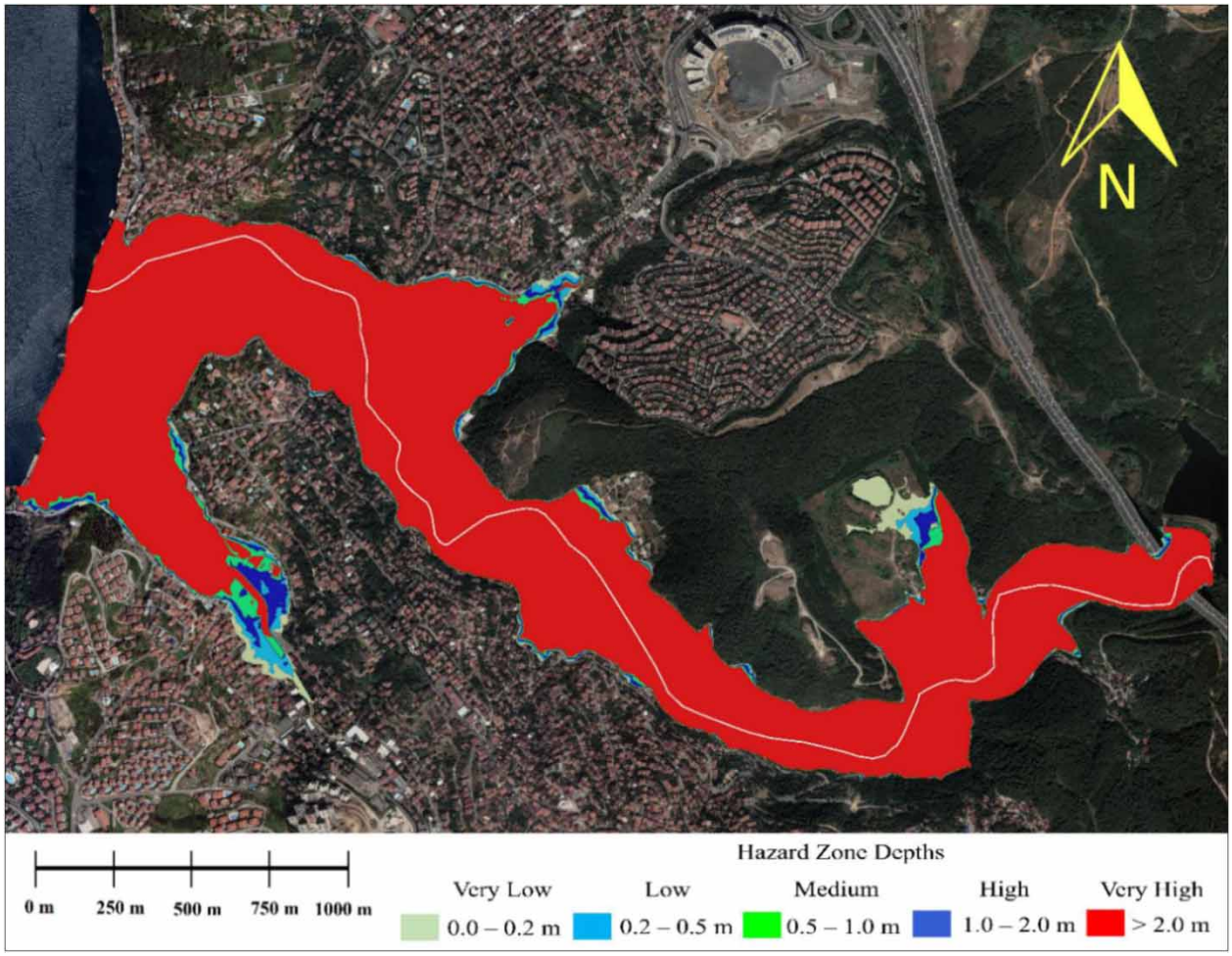

Figure 10 | Hazard zones for a dam failure.

The estimated damage costs were calculated by using the number of buildings affected by the flood, floor areas of buildings, and damage factor with respect to flood depth in our study. For this purpose, first of all, the damage factor for our study area was determined by using the flood depth obtained from the flood inundation map for the worst-case scenario and the water depth–damage factor curves obtained from the literature (Kok 2001; Penning-Rowsell 2001; Vrisou van Eck & Kok 2001; Van der Sande *et al.* 2003). The damage factor obtained by using the flood depth and water depth–damage factor curve is given in Table 4. Then, the number and floor areas of buildings affected by the flood were determined as seen in Figure 11. The floor area for a building is the sum of the ground floor area. Finally, the approximate damage costs were calculated by multiplying the floor areas of the buildings by the damage factor, the depreciation rate of buildings, and the construction cost

Table 4 | Damage costs, number of buildings affected by the flood, floor areas of buildings, and damage factor with respect to flood depth

Flood depth (m)	Damage factor	Floor areas of buildings affected by flood (m^2)	Number of buildings affected by the flood	Damage costs (₺)
0.5	0.15	2,453	18	377,235
1.0	0.18	5,409	24	734,970
1.5	0.20	4,898	19	1,064,948
2.0	0.21	13,542	63	2,301,310
3.0	0.48	19,021	61	8,958,195
4.0	0.70	7,203	23	7,633,584
≥5.0	1.00	179,554	384	260,953,800
Total cost in Turkish liras (₺)[a]: 282,024,342				
Total cost in U.S. dollars ($): 24,716,212				

[a]Property damage values in Turkish liras (₺) were converted to U.S. dollars ($) at the exchange rates on the calculation date (*source*: Turkish Central Bank, https://www.tcmb.gov.tr/; Access date: 27 December 2021).

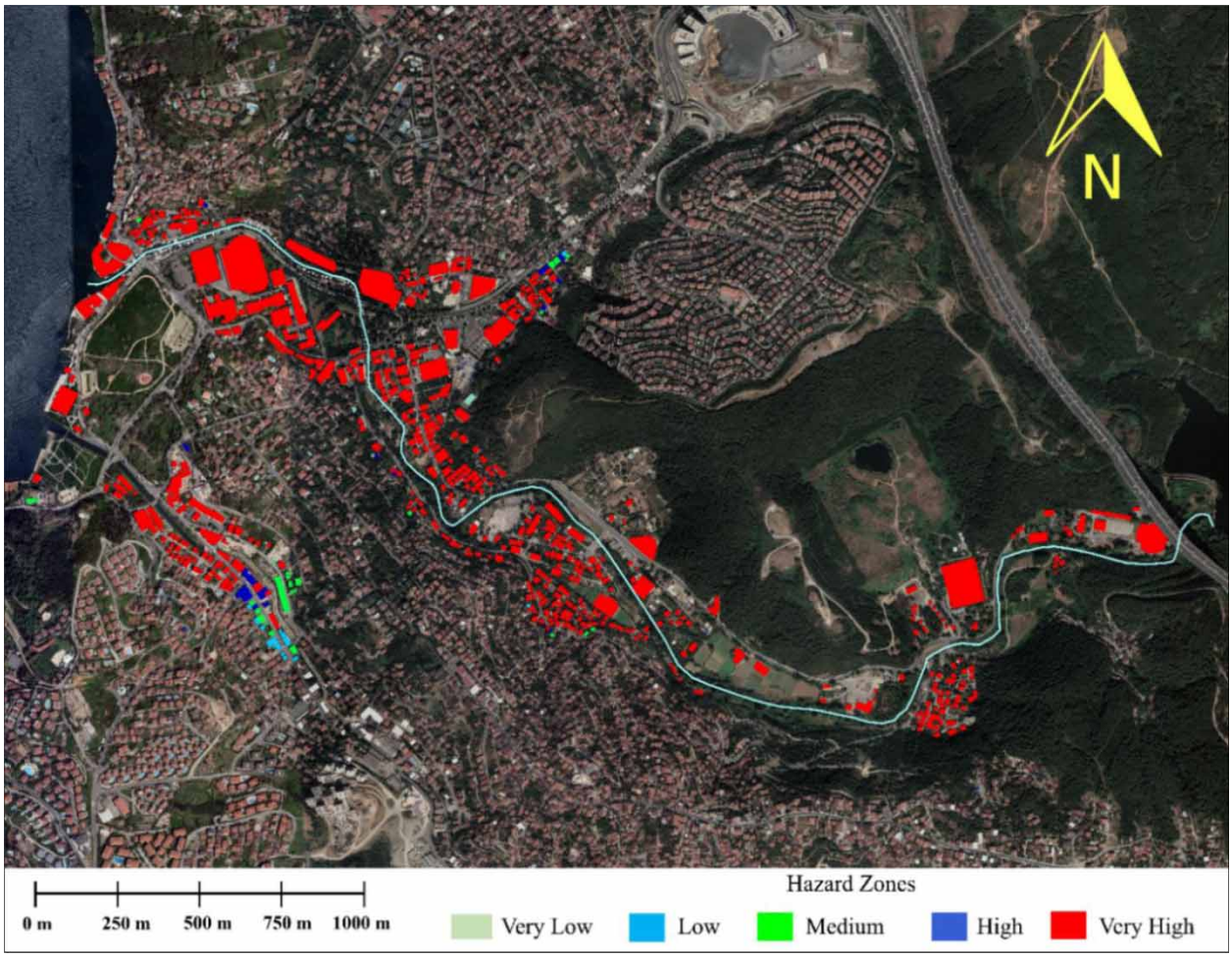

Figure 11 | The buildings affected by the flood in the hazard zones.

per unit area, which is reported by the Republic of Türkiye-Ministry of Environment, Urbanization, and Climate Change (URL-1). The calculated total construction costs in Turkish liras (₺) were converted to U.S. dollars ($) at the exchange rate of the Turkish Central Bank as shown in Table 4.

4. DISCUSSION

The potential failure of two consecutive dams, which consist of two different types of dam bodies, was analyzed in this study. Elmalı 2 concrete-buttress dam, located upstream of the consecutive dams, is important because of the structure type of its dam body and the dense-residential area located downstream. Analyzing the potential failure of a buttress dam as part of two consecutive dams causing flood risk for the high-density residential area is presented as a novel approach. Moreover, three different criteria (BFT and NFB of Elmalı 2 and RVR of Elmalı 1) were examined by simulating various scenarios to determine the impact of the dam failure on the flood-susceptible residential area.

This study reports that all dam failure simulation results affect the heavy-traffic highway and dense-residential area. Such overpopulated regions in Istanbul are of vital importance considering the harmful consequences of a possible flood disaster. In these regions, the findings obtained were evaluated in terms of the hydraulically significant peak values (peak depth, peak velocity, peak flow, and time to peak). In terms of the BFT (Criterion 1), the most dangerous scenario was determined as the sudden failure of 11 buttresses in 0.1 h. However, the scenario in which six buttresses fail for a relatively long time (0.5 h) was found to be less dangerous according to the peak values calculated. Therefore, the sudden failure scenario (0.1 h) with 11 failed buttresses is identified as the most dangerous in the analysis generated for Criterion 2. The slow failure scenario (0.5 h) with six failed buttresses was found to be less dangerous. Besides, for the cases in which Elmalı 1 was empty or full (Criterion 3), the variation in the peak values was smaller compared to the variation due to the selected factors of Elmalı 2.

For the study area, we determined that the flood depth, flow rate, and velocity can reach 15 m, 18,141 m^3/s, and 13.5 m/s, respectively, in the cross-section at the downstream area of the Elmalı 1 dam body. In addition, the results showed that the flood can reach peak flow in 13 min in the same cross-section. Moreover, the flood can reach peak flow in 22 min in the cross-section where it reaches the sea. Based on these findings, it is obvious that some precautions are required in these regions against floods due to the possible failure of Elmalı 2.

In addition, flood inundation maps for various failure scenarios of Elmalı 2 are presented. The minimum and maximum values of the three criteria were examined in the simulations with 88 runs. The differences in flood inundation areas showed the effect of the three criteria on the inundation area. According to the model results, the RVR of Elmalı 1 (Criterion 3) had no significant impacts on the inundation area. The impact of other criteria on the inundation area reached up to 14.7%. The flood inundation maps indicated that vulnerable areas with high population density can be significantly affected by possible flooding. Moreover, a flood hazard map was generated for the worst scenario. The area and the number of buildings affected by the possible failure were identified and the approximate cost of property damages in the study area was calculated. Therefore, it is of great importance to identify the areas prone to dam failure floods, to create flood inundation and hazard maps, to analyze the flood depth and velocity in the flood areas, and to determine the time to reach peak flood values. This study is believed to be helpful for the related institutions to take proper precautions, such as the installation of early warning systems, as well as the preparation of emergency and evacuation plans for people in flood-susceptible areas.

5. CONCLUSION

In this study, a dam failure analysis was performed by using HEC-RAS and various scenarios were examined. For this purpose, consecutive dams named Elmalı 1 and Elmalı 2 located upstream of the residential areas and close to a heavy-traffic highway in Istanbul, Turkey, were selected. Elmalı 2, a concrete-buttress dam located upstream of two consecutive dams, poses a flood risk for those areas. Evaluating the simulations of Elmalı 2 dam failure under different criteria such as BFT and NFB (Elmalı 2) and RVR (Elmalı 1) revealed that the study area can be seriously affected by a possible dam failure. This conclusion was reached from the peak values of hydraulically important parameters and a visual inspection of the inundation areas. Moreover, it is observed that the HEC-RAS model is useful for modeling consecutive dam systems.

The first criterion, BFT (varied between 0.1 and 0.5 h) and the second criterion NFB (varied between 6 and 11 failed buttresses) were found to be the effective criteria in flood parameters. The RVR of Elmalı 1 was determined as the less effective criterion. The water volume in Elmalı 1 did not significantly affect the flood wave caused by the possible failure of Elmalı 2. Therefore, it was determined that the operating volume of Elmalı 1 had no significant effect in preventing the adverse effects of a possible dam failure. This may be a result of the reservoir volume capacity of the downstream dam Elmalı 1 ($1.7 \times 10^6\ m^3$) being 10 times lower than the upstream dam Elmalı 2 ($17 \times 10^6\ m^3$). Elmalı 1 is operationally empty. This result shows that whether Elmalı 1 is empty or full, it is not effective in reducing the effects of flooding that may occur as

a result of any possible failure scenario. In other words, it can be argued that keeping Elmalı 1 empty may not prevent the negative consequences of the possible failure of the Elmalı 2.

The dam failure model developed is expected to provide information for flood-prone areas. The time to peak value is a crucial parameter in determining precautionary measures such as early warning systems to reduce the negative effects of a flood on residential areas. The highway is the first area to be affected by flooding and the earliest flood peak occurrence times were calculated at 13–34 min according to the dam failure scenarios examined. Determining the earliest flood peak occurrence time for a possible flood is important because this time is critical to take emergency flood response actions and to prevent life and property losses. Moreover, the flood inundation and hazard maps obtained in this study can be used to plan safe residential areas and identify buildings that need to be relocated to safe areas.

ACKNOWLEDGEMENTS

The authors would like to thank Republic of Türkiye-Ministry of National Defense General Directorate of Mapping (HGM), General Directorate of State Hydraulic Works (DSI), and Istanbul Water and Sewerage Administration (ISKI) for their data support and valuable discussions in undertaking this study. The authors would also like to express their gratitude to Dr Hasan Hüseyin Miraç Gül for his contribution to this study. The authors also would like to express their gratitude to the anonymous reviewers, the Section Editor, the Associate Editor, and the Editor for their excellent suggestions, which strengthened the paper.

DATA AVAILABILITY STATEMENT

All relevant data are included in the paper or its Supplementary Information.

CONFLICT OF INTEREST

The authors declare there is no conflict.

REFERENCES

Albu, L. M., Enea, A., Stoleriu, C. C. & Niacşu, L. 2019 GIS implementation on dam-break flood vulnerability analysis – a case study of Cătămărăşti Dam, Botoşani, Romania. In: *Air and Water Components of the Environment Conference Proceedings*, 22–24 March, Cluj-Napoca, Romania, pp. 65–76.

Albu, L. M., Enea, A., Iosub, M. & Breaban, I. G. 2020 Dam breach size comparison for flood simulations. A HEC-RAS based, GIS approach for Dracsani Lake, Sitna River, Romania. *Water* **12** (4), 1090.

Altınbilek, D. 2002 The role of dams in development. *Water Resources Development* **18** (1), 9–24.

Alvarez, M., Puertas, J., Pena, E. & Bermudez, M. 2017 Two-dimensional dam-break flood analysis in data-scarce regions: the case study of Chipembe Dam, Mozambique. *Water* **9** (6), 432.

Amini, A., Arya, A., Eghbalzadeh, A. & Javan, J. 2017 Peak flood estimation under overtopping and piping conditions at Vahdat Dam, Kurdistan Iran. *Arabian Journal of Geosciences* **10** (6), 127.

ANCOLD 2012 *Guidelines on the Consequence Categories for Dams*. Australian National Committee on Large Dams (ANCOLD), Hobart, Tasmania, Australia. ISBN:0980819253.

Aribawa, T. M., Mardjono, A., Soegiarto, S., Moe, I. R., Sihombing, Y. I., Rizaldi, A. & Farid, M. 2021 Assessment of flood propagation due to several dams break in Banten Province. *International Journal of GEOMATE* **20** (81), 185–190.

Azeez, O., Elfeki, A., Kamis, A. S. & Chaabani, A. 2020 Dam break analysis and flood disaster simulation in arid urban environment: the Um Al-Khair Dam case study, Jeddah, Saudi Arabia. *Natural Hazards* **100** (3), 995–1011.

Balogun, O. & Ganiyu, H. 2017 Study and analysis of Asa River hypothetical dam break using HEC-RAS. *Nigerian Journal of Technology* **36** (1), 315–321.

Bosa, S. & Petti, M. 2013 Overtopped the Vajont Dam in 1963. *Water Resources Management* **27** (6), 1763–1779.

Bozkus, Z. & Bag, F. 2011 Virtual failure analysis of Cinarcik Dam. *Teknik Dergi* **22** (4), 5675–5688.

Brunner, G. 2014 *Using HEC-RAS for Dam Break Studies*. U.S. Army Corps of Engineers, Hydrologic Engineering Center, TD-39, 609 Second Street, Davis, CA.

Butt, M. J., Umar, M. & Qamar, R. 2013 Landslide dam and subsequent dam-break flood estimation using HEC-RAS model in Northern Pakistan. *Natural Hazards* **65** (1), 241–254.

Cannata, M. & Marzocchi, R. 2012 Two-dimensional dam break flooding simulation: a GIS-embedded approach. *Natural Hazards* **61** (3), 1143–1159.

DHI (Danish Hydraulic Institute) 2017 *A Modelling System for Rivers and Channels (MIKE11), User Guide Manual*. DHI water and environment, Denmark.

Dinh, Q., Balica, S. & Popescu, I. 2012 Climate change impact on flood hazard, vulnerability and risk of the long Xuyen Quadrangle in the Mekong Delta. *International Journal of River Basin Management* **10** (1), 103–120.

Duchan, D., Drab, A., Riha, J., 2020 Flood protection in the Czech Republic. In: *Management of Water Quality and Quantity* (Zelenakova, M., Hlavínek, P. & Negm, A., eds). Springer Water. Springer, Cham, pp. 333–363. https://doi.org/10.1007/978-3-030-18359-2_14.

Foster, M., Fell, R. & Spannagle, M. 2000 The statistics of embankment dam failures and accidents. *Canadian Geotechnical Journal* **37** (5), 1000–1024.

Fread, D. L. 1984 *DAMBRK: The NWSS Dam Break Flood Forecasting Model*, 4th edn. Hydrologic Research Laboratory, National Weather Service, NOAA. National Weather Service (NWS) Report, NOAA, Silver Spring, MA.

Froehlich, D. C. 2008 Embankment dam breach parameters and their uncertainties. *Journal of Hydraulic Engineering* **134** (12), 1708–1721.

Haltas, I., Tayfur, G. & Elci, S. 2016 Two-dimensional numerical modeling of flood wave propagation in an urban area due to Ürkmez Dam-break, İzmir, Turkey. *Natural Hazards* **81** (3), 2103–2119.

ICOLD (International Commission on Large Dams). 1998 *Dam-break Flood Analysis – Review and Recommendations. Bulletin 111*. ICOLD, Paris.

Joshi, M. M. & Shahapure, S. S. 2017 Study of two-dimensional dam break analysis using HEC-RAS for Vir Dam. *International Journal of Engineering Technology Science and Research* **4** (8), 982–987.

Kilania, S. & Chahar, B. R. 2019 A dam break analysis using HEC-RAS. In: *World Environmental and Water Resources Congress*, 19–23 May, Pennsylvania, pp. 382–389.

Kok, M. 2001 *Stage-Damage Functions for the Meuse River Floodplain*. Communication Paper to the Joint Research Centre, Ispra, Italy.

Kumar, S., Jaswal, A., Pandey, A. & Sharma, N. 2017 Literature review of dam break studies and inundation mapping using hydraulic models and GIS. *International Research Journal of Engineering and Technology* **4** (5), 55–61.

Li, Y., Tian, C., Wen, L., Chen, A., Wang, L., Qiu, W. & Zhou, H. 2021 A study of the overtopping breach of a sand-gravel embankment dam using experimental models. *Engineering Failure Analysis* **124**, 105360.

Mahnamfar, F., Abdollahzadehmoradi, Y. & Ağiralioğlu, N. 2020 Flood risk analysis of residential areas at downstream side of Elmali Dam. *Academic Platform Journal of Natural Hazards and Disaster Management* **1** (1), 49–58.

Penning-Rowsell, E. 2001 *Stage-Damage Functions for Natural Hazards Unit. Flood Hazard Research Centre, Middlesex University, England*. Communication Paper to the Joint Research Centre, Ispra, Italy.

Petaccia, G., Lai, C. G., Milazzo, C. & Natale, L. 2016 The collapse of the Sella Zerbino gravity dam. *Engineering Geology* **211**, 39–49.

Petrascheck, A. W. & Sydler, P. A. 1984 Routing of dam break floods. *International Water Power and Dam Construction* **36** (7), 29–32.

Pilotti, M., Milanesi, L., Bacchi, V., Tomirotti, M. & Maranzoni, A. 2020 Dam-break wave propagation in alpine valley with HEC-RAS 2D: experimental Cancano test case. *Journal of Hydraulic Engineering* **146** (6), 05020003.

Qi, H. & Altinakar, M. S. 2012 GIS-based decision support system for dam break flood management under uncertainty with two-dimensional numerical simulations. *Journal of Water Resources Planning and Management* **138** (4), 334–341.

RCEM (Reclamation Consequence Estimating Methodology) 2015 *Dam Failure and Flood Event Case History Compilation*. U.S. Department of the Interior/Bureau of Reclamation, Denver, Colorado, USA.

Sawai, A., Shyamal, D. S. & Kumar, L. 2019 Dam break analysis – review of literature. *International Journal of Research in Engineering Application and Management* **4** (12), 538–542.

Sharma, P. & Mujumdar, S. 2017 Dam break analysis using HEC-RAS and HEC-GeoRAS – a case study of Ajwa Reservoir. *Journal of Water Resources and Ocean Science.* **5** (6), 108–113.

Singh, J., Altinakar, M. S. & Ding, Y. 2011 Two-dimensional numerical modeling of dam-break flows over natural terrain using a central explicit scheme. *Advances in Water Resources* **34** (10), 1366–1375.

URL-1. *Republic of Turkey-Ministry of Environment, Urbanization and Climate Change*. Available from: https://www.resmigazete.gov.tr/eskiler/2021/03/20210324-3.htm (accessed 4 December 2021).

USACE (U.S. Army Corps and Engineers) 1980 *Flood Emergency Plans, Guidelines for Corps Dams*. US Army Corps of Engineers, Hydrologic Engineering Center, Research Document No: 13, Davis, California, USA.

USACE (U.S. Army Corps and Engineers) 2016 *HEC-RAS River Analysis System, 2D Modeling User's Manual Version 5.0*. US Army Corps of Engineers California USA, Davis, CA, USA.

Van der Sande, C. J., de Jong, S. M. & de Rooc, A. P. J. 2003 A segmentation and classification approach of IKONOS-2 imagery for land cover mapping to assist flood risk and flood damage assessment. *International Journal of Applied Earth Observation and Geoinformation* **4**, 217–229.

Vrisou van Eck, N. & Kok, M. 2001 *Standaardmethode Schade en Slachtoffers Als Gevolg Van Overstromingen, Dienst Weg-en Waterbouwkunde (Standard Method Damage and Casualties Caused by Flooding, Civil Engineering Department)*. Ministry of Rijkswaterstaat, Netherlands, p. 38. 2001, publication number W-DWW-2001-028, April 2001.

Wahl, T. L. 1998 *Prediction of Embankment Dam Breach Parameters–A Literature Review and Needs Assessment, DSO-98-004, Dam Safety Research Report*. U.S. Department of the Interior Bureau of Reclamation, Dam Safety Office (DSO), Water Resources Research Laboratory.

Wahl, T. L. 2004 Uncertainty of prediction of embankment dam breach parameters. *Journal of Hydraulic Engineering* **130** (5), 389–397.

Wu, W. 2011 Earthen embankment breaching. *Journal of Hydraulic Engineering* **137** (12), 1549–1564.

Xiong, Y. 2011 A dam break analysis using HEC-RAS. *Journal of Water Resource and Protection* **3** (6), 370–379.

Yakti, B. P., Adityawan, M. B., Farid, M., Suryadi, Y., Nugroho, J. & Hadihardaja, I. K. 2018 2D modeling of flood propagation due to the failure of way Ela Natural Dam. *MATEC Web Conference* **147**, 03009.

Yu, S., Zhang, Q., Chen, Z., Hao, J., Wang, L., Li, P. & Zhong, Q. 2021 Study of the sheyuegou Dam breach – experience with the post-failure investigation and back analysis. *Engineering Failure Analysis* **125**, 105441.

Zhang, L. M., Xu, Y. & Jia, J. S. 2009 Analysis of earth dam failures: a database approach. *Georisk: Assessment and Management of Risk for Engineered Systems and Geohazards* **3** (3), 184–189.

First received 25 November 2022; accepted in revised form 5 February 2023. Available online 21 February 2023